Life Support & Biosphere Science, Vol. 8 pp. 43-53
1069-9422/01 $20.00+ .00

AN OPTIMAL CONTROL STRATEGY FOR CROP GROWTH IN ADVANCED LIFE SUPPORT SYSTEMS

DAVID H. FLEISHER* and HAIM BARUHf

*Department of Plant Biology and Pathology, Rutgers, the State University of New Jersey,
20 Ag Extension Way, New Brunswick, NJ 08901-8500
f Department of Mechanical and Aerospace Engineering, Rutgers,
the State University of New Jersey, 98 Brett Road, Piscataway, NJ 08854-8058

A feedback control method for regulating crop growth in advanced life support systems is presented. Two models for crop growth are considered, one developed by the agricultural industry and used by the Ames Research Center, and a mechanistic model, termed the Energy Cascade model. Proportional and pointwise-optimal control laws are applied to both models using wheat as the crop and light intensity as the control input. The control is particularly sensitive to errors in measurement of crop dry mass. However, it is shown that the proposed approach is a potentially viable way of controlling crop growth as it compensates for model errors and problems associated with applying the desired control input due to environmental disturbances.

Biomass production Mathematical modeling Advanced life support Feedback control
Model-based control

INTRODUCTION

Future manned space exploration will require life support systems that are independent of the Earth for resupply of food and resources. Integrated physical, chemical, and biological systems may provide mass closure for life support through recycling and recovery of system resources via waste processing, atmospheric purification, and food production for crew members from plant biomass production chambers. NASA (National Aeronautics and Space Administration) researchers are developing aspects of this system through the ALSS (Advanced Life Support Systems) project (13,16,18,22).

Plant growth is expected to play an important role in ALSS. Growth of higher plants provides crew members with food, potable water via transpiration, atmospheric gas exchange through photosynthesis, and a contribution to waste processing/resource recycling through hydroponic nutrient uptake. A mix of 8 to 14 crops is required to satisfy crew nutrition demands (17). Crops in an ALSS environment will most likely be hydroponically growth in individualized growth chambers with control over irradiance (photosynthetic photon flux or PPF), photoperiod, air temperature, relative humidity, atmospheric carbon dioxide and oxygen concentrations, and nutrient delivery system quality (3). The environmental setpoints for each of these inputs should be selected to produce the desired levels of plant growth that satisfy ALSS crop production scheduling (i.e., timing and yield of each crop). Production sched-

Address correspondence to David H. Fleisher, Bioresource Engineering, Rutgers, the State University of New Jersey, 20 Ag Extension Way, New Brunswick, NJ 08901-8500. Tel: (732) 932-9753; Fax: (732) 932-7931; E-mail: fleisher@bioresource.rutgers.edu

ules would initially be derived from crew nutrition demands. Disturbances and system failures can influence plant production in a closed environment. These include poor crop seed germination, spread of plant pathogens and/or disease, and perturbations in environmental conditions in the growth chamber (12). Environmental perturbations can be of either short (less than 1 day) or long-term duration, and may ensue from deliberate actions (to modify plant transpiration or photosynthetic rates to offset activities in other ALSS compartments, for example) or system failures (such as fluctuations in power availability or mechanical problems). In either case, crop growth, and hence production scheduling, may be adversely affected by environmental perturbations. For example, a long-term reduction in the light intensity or atmospheric carbon dioxide concentration can lower photosynthetic rates and potentially decrease crop growth rates. Air temperature perturbations can affect growth and carbohydrate partitioning, and may delay or increase plant developmental rates depending on the duration, magnitude, and time during the crop life cycle at which the disturbance occurs (15,26). Environmental disturbances can negatively affect reliability and persistence issues for an ALSS system (14).

Control strategies able to compensate for the effects of environmental perturbations on plant growth would be useful for ALS. However, most growth chamber controllers work to maintain static setpoints. These setpoint values are typically derived from heuristic knowledge and empirical studies for each particular crop [for example, see (6,7,19)]. As a result, environmental control of growth chambers tends to concentrate on maintaining current setpoints at their predetermined levels; thus, environmental disturbances and their effects on the plant are not incorporated into the control.

Optimization techniques have also been used to identify appropriate setpoint values. Modern greenhouse control integrates mathematical models of the greenhouse environment with simple plant growth models to prescribe daily environmental conditions. The results are management tools and control systems that dynamically determine optimal setpoints to increase crop yield, quality, or decrease energy consumption [e.g., (1,2,8,9,23,24)]. Chun and Mitchell (10) developed a dynamic controller that varied PPF to control lettuce canopy net photosynthesis in a growth chamber based on real-time measurements of canopy gas exchange. In this case, the environmental input was dynamically varied so that the desired plant growth rate could be obtained. Such systems could be adapted for ALS use, where controllers could maintain both setpoints and adjust them when necessary based on measured or predicted properties of the crop. Measurement errors and uncertainties in the mathematical models would need to be considered in developing this control.

In this article, we propose to use feedback control to compensate for the effects of environmental disturbances in crop growth chambers by adjusting PPF to maintain desired crop growth rates. We consider two generic crop growth models and we develop two model-based feedback controllers, using wheat as the crop. Small-order mathematical errors are considered. The controllers are evaluated with several scenarios simulating short-term environment perturbations and control system errors.

CROP GROWTH MODELS

In order to apply model-based control laws, we need to make use of crop growth models. In this article, we consider two such models. The first is a growth and assimilation model, developed by the agricultural industry and used by the NASA Ames Research Center for previous ALS studies (4). The second model is called the Energy Cascade model (27), which takes a more mechanistic approach to predicting crop growth and overcomes some of the shortcomings of the Ames model. Both models assume a linear relationship between light intensity and crop growth rate.

Ames Model

Originally developed by three agricultural companies (General Mills Inc., PhytoFarms of America, and CEA Technologies International, Inc.), this model has been utilized to study production systems for several crops including lettuce, spinach, wheat, and tomato. NASA's Ames Research Center has also applied the model towards design of environmental bioregenerative life support systems (4).

Relative growth rate (time rate of change of plant dry mass per unit of current dry mass) is predicted as a function of photosynthetic photon flux (PPF), carbon dioxide concentration (CO_2), air temperature (7), plant production area, plant parameters (quantum use efficiency, canopy architecture), and initial plant dry mass as:

$$G_r = W_r \, a_1 - 1 - e \qquad (1)$$

where

G.: relative growth rate (g g~' • time*[1] • nr[2])

C: canopy quantum use efficiency (g biomass mol"[1] intercepted photons)

E: nondimensional environmental response surface (for CO_2 and *T),* between 0 and 1

P:. integrated incident PPF over simulation time increment *i* (umol rm[2] • time"[1])

W.: crop dry mass (g)

a: fraction of *P.* intercepted by plant canopy (between 0 and 1) plant spacing (m^2)
crop canopy constant (area of ground covered by plant canopy per plant dry mass, m^2 g'")
simulation time increment (day)

The plant dry mass is determined as:

— wo"1 (2)

The model can be iterated on daily or smaller time increments. Control of crop growth can be achieved via manipulation of photoperiod and light intensity, which contribute to the light integral for the given time step. The model is terminated at a user-specified plant maturity date.

Energy Cascade Model

The energy cascade model (27) predicts crop productivity during plant growth and development based on a three-step analysis involving: 1) light absorption *L,* where a fraction of photosynthetically active radiation available to the crop is absorbed by the canopy; 2) canopy quantum yield *Q* (mol carbon mol~' PPF), the conversion of absorbed light energy into carbon via photosynthesis; 3) carbon use efficiency *U* (mol C mol"[1] C), the fraction of the quantum yield that is incorporated into plant biomass.

The model combines the above energy cascade process to predict gross and net photosynthesis *(P* and P_n), daytime respiration *(R),* and crop growth rate (CGR) as follows:

(3)

To compute the daily crop growth rate, nighttime respiration needs to be taken into account. Thus, CGR is equal to the daily net photosynthetic rate *(HP_m),* where *H.* is the photoperiod, minus plant respiration occurring during the dark [(24 - //.)/?.] as:

p(ff,.P_w.- (24 -#,>,.) (4)

Dry mass is then calculated as:

(5)

with variables and units defined in Table 1.

Unlike the Ames model, the energy cascade model also simulates the effect of senescence by incorporating time dependence with the value for quantum use efficiency as:

$$Q_i = \begin{cases} Q_a & for\ i < i_a \\ & for\ i > i_q \end{cases} \quad (6)$$

where 2_{max} and $<2_{min}$ are th[£] maximum and minimum quantum yield values for particular experiment (in mol carbon mol"[1] PPF), i_m is the time to crop maturity (days), *i* is the time at which quantum yield begins to decline (days), and *i* is the simulation time increment (day).

Canopy growth and development are indirectly simulated with a linear increase in light absorption *L* until a constant maximum value of light absorption *(L_{mK})* is achieved according to

$$L, = \begin{cases} L, & for\ i < i_t for\ i > i, \end{cases} \quad (7)$$

where L^ is the maximum fraction of light absorbed at canopy closure (between 0 and 1) and $i_($ is the time at which canopy is completely closed (in days).

Model applications are restricted to the environmental ranges, plant cultivars, and planting densities from the data sets from which it was developed. Constant values are entered in the model for L , *Q* , *Q* . , *U, i,, i,* max' ^max' ^mm' ' /' 9' and i_m. The model accepts light intensity as an input.

Variable .. List of Symbols

Ames Model terms	Description
W	plant dry mass (g)
·	canopy quantum use efficiency (g mol"[1] intercepted photons)
E	nondimensional environmental response surface
5,	plant spacing (m^2)
G!	relative growth rate (g g"[1] • time"' • m"[2])
P.	integrated PPF (umol m"[2] • time"[1])
a.	fraction of P. intercepted by plant canopy (0 to 1)
k	crop canopy constant (m^2 ground g"' plant)

Energy Cascade Model terms	
P	gross photosynthesis (umol CO, nr^2 • s"[1])
P	net photosynthesis (umol CO, m"[2] • s"')
R	daytime respiration (umol CO_2 m"[2] • S"[1])
CGR	crop growth rate (g $m\sim^2$-d"')
W_i	plant dry mass (g nr^2)
i	time of maturity (days)
i	time of onset of senescence (days)
3	conversion factor*
H	photoperiod (h)
Z,	fraction of light absorbed (0 to 1)
U	carbon use efficiency (mol C mol"[1] C)
Q	maximum quantum yield (mol C mol PPF"')
Q^	minumum quantum yield (mol C mol PPF"')
i(	time of canopy closure (days)

Control terms	
x	state (system) vector (=W.)
x_f	desired values for state vector (=Wj,)
u,	control vector (=/",)
y(	output vector (=W.)
y^.	desired values for output vector (=W_d)
J_M	performance index
[A,]	state matrix
[BJ	input matrix
[C,]	output matrix
[K.]	control gain matrix
[HJ,[/y	error and control weighting matrices
e_M	error vector

*3 = 0.098 obtained by multiplying 10-[6] mol CO_2 umol"' C0., 12 g C mol-' CO_2, 2.27 g biomass g"[1] C, and 3600 s h"' as in Volk et al. (27).

CONTROLLER DEVELOPMENT

In this section, we construct a model-based crop growth controller. The input to the controller is taken as the PPF and the output is plant dry mass. Consider a system described by the discrete time equations

(8)

in which *i* denotes the time step, *x.* is the system vector of order *n*, describing the *n* states of the system, *u.* is the control vector of order *m*, corresponding to *m* control inputs, and *y.* is the output vector, denoting the measured states. The matrices..[A], [S.], and [C] describe the properties of the state, the relation of the controls to the state, and the relation between measured values and the state variables, respectively (Table 1).

The equations above can represent a discrete system or they can be descriptive of a discretized model. In the latter case, the time increment should be selected such that the accuracy of the actual model is not compromised.

Denoting the desired values of the output variables as y_d. ($i = 1, 2, \ldots$), we first consider proportional control. Here, one designs the control input as

(9)

where [K] is the control gain matrix and $z_i = [B]\sim^J(x_t$ - [A.];^.). The gain matrix is selected such that the closed loop system matrix ([A.] - [5.][£.][C.], $i = 1, 2, \ldots$) describes a stable system; that is, its eigenvalues lie within the unit circle. The procedures we use to select the control gains will be described later.

Another control approach is based on pointwise-optimal control (25). The objective of pointwise-optimal control is to drive the system to a desired set of values and to do this by minimizing the difference between the measured variables and their desired quantities at each time step. Unlike conventional optimal control, which minimizes the difference between a desired state and an initial state over a period of time, pointwise-optimal control does this at each time step. The result is a simpler, but a less sophisticated, control law.

We wish to minimize the difference between y_{di} and >•. at each time increment. To this end, given the measurements at time step *i*, we predict the state at the next time increment ($i + 1$) using eq. (8) and we define a performance index as

$$J_M - CM\,[HU_{+i}\,k+i^{+M}f\,[\hat{}21\,K \qquad W)$$

where e_M is the error vector between the desired and actual values of the output,

(11)

with [Hj] and $[H_2]$ as weighting matrices. The performance index is a measure that weighs the error versus the control effort. Setting [//J to zero implies that one can use as much control effort as needed, without regard to the amount used. To minimize the performance index, we take the derivative of J_M with respect to *u.*

$$\frac{dJ_M}{dU_:} \qquad (12)$$

where , = -[C.+1][fi.]. Setting eq. (12) equal to zero and solving for *u.*, we obtain

in which [/y = [/g + [5,HC J^r[#$_{li+1}$][C$_w$][B.]. Equa-tion (13) has x in it, which implies that if [C.+1] is not a square matrix (not as many measurements as there are states) an observer needs to be designed to estimate *x.* from *y.*. The same situation exists when proportional control is used.

Both control laws can be applied to the two crop models. Both mathematical models are of order $n = 1$ and there is one controller, $m = 1$. For now, we assume that the state variable W, the dry mass, can be directly measured so that [C] is a scalar and it is equal to 1. To obtain [A.] and [£.], which are also scalars, we recognize that both models must be in the state space form given by eq. (8). (Note that the notation [-] will now be dropped because the matrices are scalars for this application.)

Consider the Ames model [eq. (2)], where dry mass is an exponential function of relative growth rate, *G.*.

The first-order Taylor series expansion of e^c< is

(14)

which is an accurate approximation when G. is kept sufficiently small. This can be accomplished by reducing the model's time step to a 0.2-day period. Values for G. simulated in the model do not exceed 0.7 per day. By utilizing a 0.2-day time period, the maximum simulated value is reduced to 0.14 and the resulting error due to linearization is 0.9%. Because we are designing a feedback controller and the dry mass *W.* is measured at every time increment (1 day), each approximation is carried out for 1 day only. That is, the control is to be applied at the end of each day of simulation, not at the 1/5 day time increment. Hence, errors associated with this approximation do not increase with time.

In eq. (1), exponential of the plant dry mass divided by the plant spacing is computed to determine the fraction of light intercepted by the plant canopy, *a.*. In this case, the linearization expansion cannot be performed accurately because the dry mass continually increases throughout the simulation. This turns out to not be a drawback when designing the control law.

Combining eqs. (1), (2), and (14) gives the following expression for crop dry mass:

(15)

which now is in desired form, with $x. = W.$, $A. = 1$, $B. = CEa.$, $C. = 1$, and «. = />..

CONTROLLER IMPLEMENTATION

In this section, we implement two control laws described above for the Ames and Energy Cascade models. We consider the following issues: a) The type of control law (proportional or pointwise-optimal); b) the crop model on which the control design is based; c) the crop model that is used to simulate crop dry mass; d) presence of measurement as well as control input errors.

For example, one procedure is to simulate the plant state via the Energy Cascade model, while designing the control law based on the Ames model. The reasoning behind this approach is to see if a controller based on one model can effectively control a different model. As the models of crop growth considered here are simplifications of complex phenomena, one needs to design a controller that has certain robustness features and one that will work with different models describing the same phenomena. Using more than one model to describe the same system is a common procedure for control system development (5) and is frequently done in the life sciences.

Applied Control Law Expressions

The weighting matrices in the pointwise-optimal control law become scalars H$_{lj+1}$ and H_y when applied to the

crop models considered here. Introducing all the coefficient terms used to derive the previous equation into eq. (15), the control input for the Ames model becomes

$$= p. =\bullet \quad (16)$$

In general, the values for H_{IM} and //,. are selected by trial and error. Appropriate values for these matrices are discussed later on in this section. For the special case of no restrictions on the control effort, we can set H_{2i} to zero and selecting $H_{IM} = 1/CEA.$, we obtain

$$P_i = \frac{W \quad -W}{CE\left(1-e^{-k\frac{W_i}{S_i}}\right)} \quad (17)$$

Note that the above equation can also be derived directly from eq. (11), by prescribing that the difference between W_{dM} - W_M be zero.

Basing the control design on the Energy Cascade model, and without putting a restriction on the control effort in the control design, we obtain a pointwise-optimal control law in the form

$$P, = \quad ' \quad BQ_iL_i(H_{\cdot}+24(U-24)) \quad (18)$$

Finally, the proportional control law [eq. (9)] as applied to the Ames model is

$$CEa, \quad (19)$$

A similar expression can be derived for the Energy Cascade model.

Identification of Control and Simulation Model

Simulations with the Energy Cascade and partially linearized Ames models were conducted prior to implementing feedback control. Baseline environmental conditions for simulation were set at a carbon dioxide concentration of 1200 ppm, a PPF level of 1400 umol $nr^2 \cdot s"^1$, a 296°K constant day/night temperature, photoperiod of 20 h, and a production area of 700 plants nr^2. These parameters were taken from Volk et al. (27) for the Energy Cascade and then fit to the Ames model (Table 2). Model simulations of wheat growth were similar until day 33, when productivity declined in the Energy Cascade model due to senescence (Fig. 1). This result has important consequences when determining which model to use for simulation and for the control law.

Four separate simulations were performed to determine which model to use for control and for simulation. The simulations were 1) Ames-based controller with Energy Cascade model for dry mass prediction, 2) Ames-based controller with Ames model for dry mass prediction, 3) Energy Cascade based controller with Energy Cascade model, and 4) Energy Cascade based controller with Ames model. Each simulation used the same set of desired dry mass values, W_{dM} (i - 1,2,..., 66). Desired values were generated from a simulation with the Energy Cascade model under the baseline conditions discussed above with a setpoint PPF of 1400 umol $nr^2 \cdot s\sim'$. The controller's response was restricted to a PPF range between 50 and 2000 umol $nr^2 \cdot s"^1$ PPF, where wheat response to changes in light intensity was assumed linear (21). Simulation results were judged on the controller's ability to achieve the desired plant mass values and feasibility of output PPF level; effects of environmental perturbations were not evaluated at this stage.

All four combinations were able to maintain the desired plant dry masses throughout the simulation. However, when the Ames model was used for simulation of crop growth, input PPF values were well below the

Table 2. Values for Energy Cascade and Ames Models

Energy Cascade Model	
$L^\wedge$ (unitless)	0.93
$Q^\wedge$ (mol C mol PPF^{-1})	0.0625
Q^{TM} (mol C mol PPF^{-1})	0.0125
U (mol C mol C^{-1})	0.68
i, (days)	12
', (days)	33
i_a (days)	62
Ames Model	
C (g mol $photon"^1$)	1.12
k (m^2 ground g-')	100
E (unitless)	0.85
W (g)	0.001
S, (m^2)	14.3

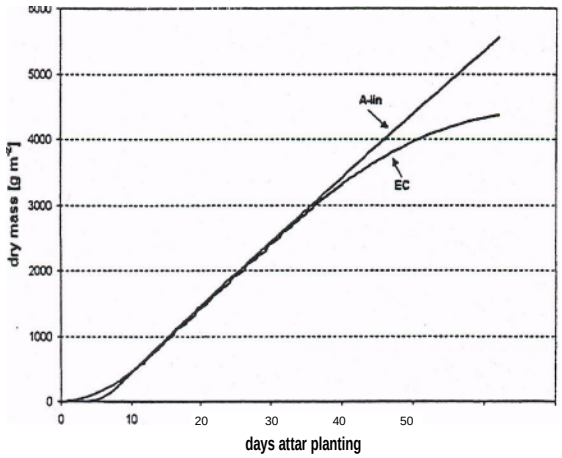

Figure 1. Comparison of Energy Cascade (EC) model versus partially linearized Ames model (A-lin) for wheat dry mass over time.

expected value of 1400, particularly at the start of senescence. For example, when the control law applied to the Energy Cascade model was used [eq. (18)], PPF values following DAP 33 averaged 847 umol $m^{-2} \cdot s^{-1}$. This occurred because the Ames model does not simulate the decline in plant productivity following the onset of senescence. The Ames model overpredicted plant dry mass, and the controller supplied lower PPF values to compensate.

Using either the Energy Cascade or Ames models for the control and the Energy Cascade model for the simulation produced similar results. For brevity, our subsequent analysis is based on using the Ames-based control law [eq. (17) or eq. (19)] with the Energy Cascade model for simulations.

Control Implementation

Simulations using the Ames-based pointwise-optimal control law [eq. (17)] showed that the PPF oscillated wildly during different days of the simulation. This was because our control design did not weight the control effort (i.e., H_2. was assigned a value of 0). This is undesirable for two reasons. First, the control action is not smooth, which usually leads to high sensitivity to changes in parameters and instabilities in the control action. Second, such a control action will put large fluctuating demands on the power supply in the ALSS environment, which may result in a reduction in power allocated to other components of the ALSS. These considerations suggest that values for the control gain needed to be determined.

Simulations were conducted to determine parameters for proportional control, *K.*, and weighing terms H , E_v for pointwise-optimal control. The results were evaluated in terms of system response and required control effort. A normalized least squares criterion was introduced to quantify control effort and the cumulative deviation from desired set points over the entire simulation. The criterion evaluates the deviation in dry mass *W* as well as the control input PPF, and it has the form

$$LS = \pm\pm \qquad (20)$$
$$LS_{7,}$$

where

Z: represents either dry mass *WOT* light intensity PPF

$Z_{s.}$: 62: nominal setpoint at time increment *i* (e.g., 1400 when Z = *P.* or $W_{d.}$ when *Z* - W.)

$Z_{max'}$ number of days in simulation (equals crop maturity date)

maximum least squares value observed from all simulations

Smaller LS_Z values imply less deviation from nominal or desired values.

For proportional control, the control gain *K.* was selected so that the eigenvalue of the closed loop system lay within the unit circle. This requires that values for *K.* be negative. For pointwise-optimal control, H_{tM} was kept equal to *ICEa.* as in eq. (17), but $H_{2.}$ was set as a percentage of H_{li+l}- Separate simulations were run with proportional and pointwise-optimal control laws to determine appropriate constants for these parameters.

For both proportional and pointwise-optimal control simulations, least square values for system response were similar regardless of trial values selected. However, the amount of control effort varied greatly depending on the control gain selected. Figure 2 shows LS_Z results for PPF $(LS_{?pf})$ for different proportional control gain values. It can be seen that a value of-0.6 (held constant throughout the simulation) minimized PPF fluctuations. For pointwise-optimal, $H_{2.}$ set to 350% of H minimized $L\ S$.

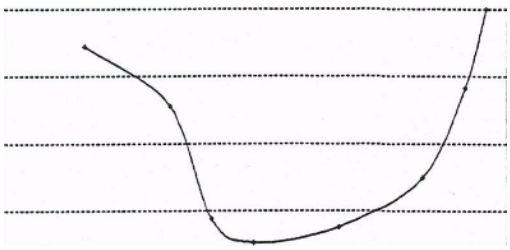

Figure *2.* Effect of gain value for Ames-based proportional controller on control effort.

Using the best values of the control gain parameters, the predicted plant growth and input PPF for pointwise-optimal control and proportional control were compared. Table 3 summarizes the results for the normalized least square values in plant growth and PPF for a variety of disturbances and for the two control laws considered. Disturbances consisted of ±40%, 20%, or 10% short-term changes to the input PPF. Short-term disturbances were implemented from days 11 to 20 for single disturbances and from days 11 to 15 and 31 to 35 for double disturbances. Figure 3a and b compares control input over time between the two controllers for single and double disturbances.

Using only the pointwise-optimal controller, four additional simulations were performed where ±40% and 20% perturbations were maintained throughout the simulation. These simulations were conducted to determine the ability of the controller to respond to long-term disturbances. Long-term measurement errors (±20% of W.) were also input to the controller in separate simulations. Results are also summarized in Table 3. Figure 4a and b shows results from long-term -40% and short-term -40% perturbations, respectively.

DISCUSSION

The results in Table 3 indicate that the proportional and pointwise-optimal controller performances are comparable in terms of maintaining desired plant dry masses. However, proportional control shows slightly more sensitivity to input disturbances, as can be seen in Figure 3 and the larger LS_{ppf} values in Table 3. This higher sensitivity is a disadvantage. Large fluctuations in input PPF may lead to a reduction in the energy supplied to other components of the ALSS system and decrease longevity of the growth chamber lighting sys-

Table 3. Normalized (0 to 1) Least Square for Plant Growth *W.* and PPF for Different Scenarios and Percent Final Deviation From Desired Plant Mass at Maturity Date (Reported for Pointwise Control Only)

Proportional			Pointwise		
Scenario	W	PPF.	*W.*	PPF.	%
+40% PPF, 10	0.140	0.732	0.173	0.723	2 (8.6)
-40% PPF. 10	0.273	0.671	0.289	0.570	2 (9.2)
+20% PPF. 10	0.0749	0.463	0.128	0.473	2(4.1)
-20% PPF. 10	0.156	0.512	0.188	0.345	2 (4.8)
+10% PPF. 10	0.0683	0.356	0.126	0.325	2(2)
-10% PPF. 10	0.111	0.403	0.153	0.227	2 (2.6)
+20%. -10%. 5	0.0665	0.365	0.139	0.376	2
-20%. +10%. 5	0.098	0.653	0.152	0.341	2
+40% PPF. long	—	—	0.129	0.701	1.4
-40% PPF. long	—	—	1.0	0.825	19
+20% PPF. long	—	—	0.147	0.73	1.6
-20% PPF. long	—	—	0.229	0.742	2.5
+20% IV. long	—	—	0.85	0.829	18
-20% *W.*, long	—	—	0.954	0.972	22

The values in parentheses are percent deviation from desired at maturity when no control action is applied.

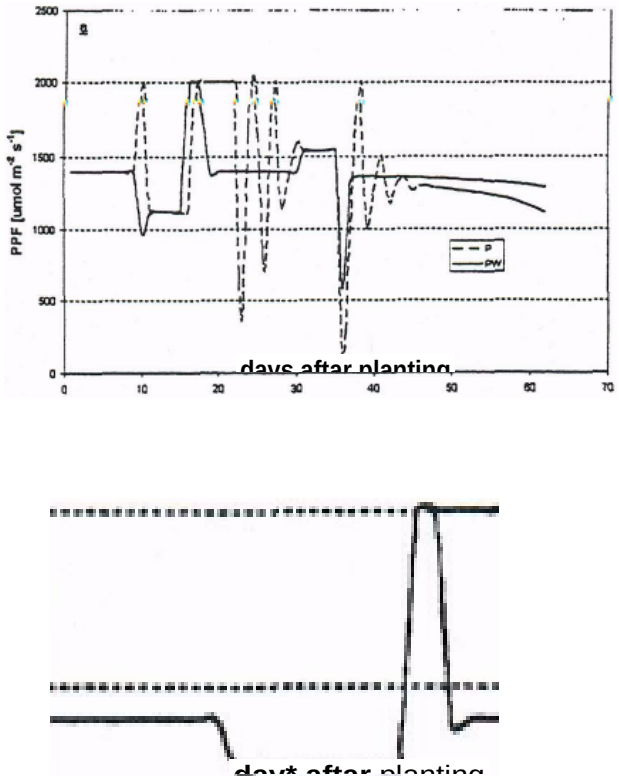

Figure 3. Control effort comparisons between proportional (P) and pointwise-optimal (PW) controllers. Examples shown are for-20%, +10% (a) and -10% short-term perturbations (b).

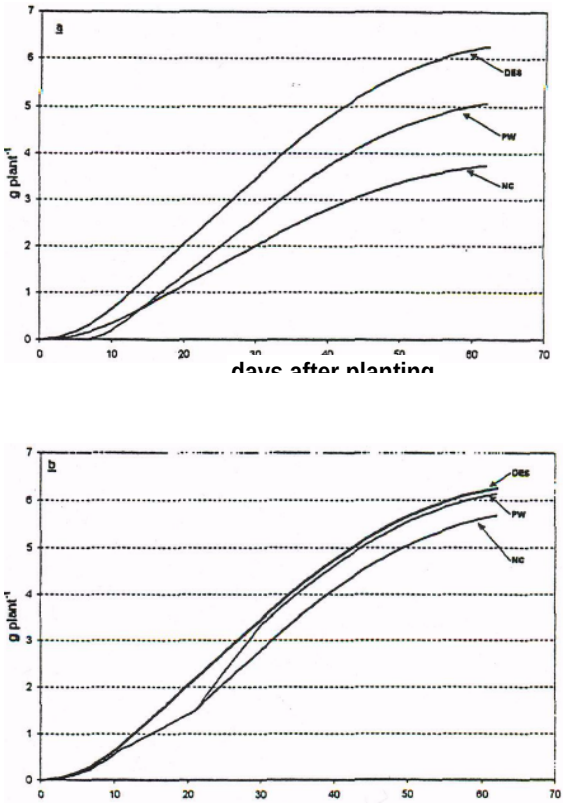

Figure 4. System response *(W)* from pointwise-optimal controller for -40% long-term perturbation (a) and -40% short-term perturbation (b). Simulated control values (PW) are compared with desired dry masses (DES) and results in which no control is applied (NC) to adjust for the perturbation.

terns. The even distribution of energy and avoidance of excess variations in power demands will be an important concern as ALSS subsystems are integrated (11). For this reason, the pointwise-optimal controller was shown to be a better controller choice for this application.

The short-term disturbances introduced to the pointwise-optimal controller represent a range of some possible external perturbations to light intensity. The controller was able to compensate for all short-term disturbances in PPF (Fig. 4b), as well as small (20%) long-term disturbances (Table 3). However, for a long-term perturbation of *-40%* PPF, predicted final dry mass ended 19% below its desired value. This occurred because PPF output was restricted due to the constraints set on the control law. Thus, the crop could not be restored to the original production schedule when a -40% disturbance was applied during the entire simulation (Fig. 4a). This implies that the simulation results are dependent on both the PPF setpoint and the PPF range constraints placed on controller response.

Table 3 also shows the resulting final dry mass errors for each short-term scenario when no controller action was applied (last column, in parentheses). That is, following the perturbation, PPF was set back to the nominal value of 1400 fimol nr^2 • s~'. Errors ranged from about 10% to 2%. These deviations were reduced to less than 2% with the controller (Fig. 4b shows the short-term -40% result). It is worth noting that as the duration of perturbation increases, the deviations will increase. Thus, for short-term and certain long-term perturbations, utilization of a controller to restore crops back to their original production schedule is a viable and necessary approach.

Useful real-time, nondestructive measurements of crop dry masses are not currently achievable. Hence, needs to be developed to estimate the crop dry mass in a nondestructive way.

In a real-time application, crew members would input environmental perturbations to an observer to estimate the current dry weight *W*.. This estimated dry mass would then be used as the input to the controller. To investigate the sensitivity of the control action to incorrect measurements of the dry mass, the controller was evaluated for when values for dry mass *W*. in eq. (17) were perturbed by ±20%. As listed in Table 3, controller response is adversely affected by errors in the estimated dry mass. We conclude that an accurate estimation of W. is critical to the controller's ability to compensate for environmental perturbations and is an important topic for research.

Ultimately, the development of dynamic controllers, such as the one presented here, for individual ALS processes will need to be considered as subsystems are linked together. The simple method presented here is intended to outline one viable approach of developing such control for biomass production. There are several areas where the control design requires improvement. The controller is based on a single input, single output model. More realistic controllers will have to handle multiple inputs, include carbon dioxide concentration, temperature, photoperiod, and microgravity. An improved model should also account for the nonlinear relationship between light intensity and growth rate. For example, constants that are fixed in the Energy Cascade model are actually dynamic functions of the environment. Values for $<2_{raax}$ and *U* depend on the current temperature, light intensity, and CO concentration, while photoperiod affects developmental parameters such as maturity and canopy closure dates. Jones and Cavazzoni (20) have recently demonstrated that such affects may be incorporated in simple crop models by parameterizing certain variables in the Energy Cascade model. Incorporating these relationships into the control algorithm will be important. An accurate observation scheme for estimating values of the crop dry mass nondestructively will need to be developed for true feedback control. Growth chamber experiments would then be implemented to validate the results predicted by the controller.

CONCLUSIONS

A model-based feedback controller is developed to maintain crop production schedules in advanced life support systems, where perturbations in light intensity and measurement of crop growth rates may be of control laws are developed. The control laws are applied to two plant growth models and wheat is used as the crop. The response is evaluated with several "what-if' scenarios including simulated short- and long-term errors in the input for light intensity. The control was shown to be particularly sensitive to errors in measurement of plant dry mass. However, the controller satisfactorily responds to small perturbations in light intensity, making feedback control a viable option to regulate crop growth systems in space missions.

ACKNOWLEDGeMENTS

This project was supported by the NJ-NSCORT (New Jersey-NASA Specialized Center of Research and Training) and a NASA Graduate Student Researchers Program fellowship (#NGT5-50229). New Jersey Agricultural Experiment Station Paper #D-70501-13-01.

David Fleisher is an assistant professor of Plant Science. He has a M.S. degree in Bioresource Engineering and an interdisciplinary Ph.D. in Bioresource Engineering, Mechanical and Aerospace Engineering, and Plant Science from Rutgers University. His research interests include systems analysis, modeling, sensing and imaging, and control for controlled environment plant production.

Haim Baruh is an associate professor in Mechanical and Aerospace Engineering. He has a M.S. and Ph.D. in Engineering Mechanics from Virginia Polytechnic Institute and State University. His research interests include modeling and control of elastic structures, control of agricultural systems, and dynam-

REFERENCES

1. Aaslyng, J. M.; Ehler, N.; Karlsen, P.; Rosenqvist, E. Intelligrow: A component-based climate control system for decreasing greenhouse energy consumption. Acta Hort. 507:35^*2; 1999.
2. Aikman, D. P. A procedure for optimizing carbon dioxide enrichment of a glasshouse tomato crop. J. Agric. Eng. Res.63:171-184; 1996.
3. Barta, D. J.; Castillo, J. M.; Forston, R. E. The biomass production system for the bioregenerative planetary life support systems test complex: Preliminary designs and considerations. SAE Technical Paper No. 1999-01-2188. Warendale, PA: Society of Automotive Engineers; 1999.
4. Bates, M. E.; Bubenheim, D. L. Applications of process control to plant-based life support systems. SAE Techni-

cal Paper No. 972359. Warrendale, PA: Society of Automotive Engineers; 1999.
5. Blackwell, C. C; Blackwell, A. L. CELSS system control: Issues, methods, and directions. Adv. Space Res. 12(5):57-63; 1992.
6. Bugbee, B.C.; Salisbury, F. B. Current and potential productivity of wheat for a controlled environment life support system. Adv. Space Res. 9(8):5-15; 1989.
7. Bugbee, B. G.; Salisbury, F. B. Exploring the limits of crop productivity: Photosynthetic efficiency of wheat in high irradianceenvironments. Plant Physiol. 88:869-878; 1988.
8. Challa, H. Integration of explanatory and empirical crop models for greenhouse management support. Acta Hort. 507:107-116; 1999.
9. Challa, H.: van Straten, G. Optimal diurnal climate control in greenhouses as related to greenhouse management and crop requirements. In: Hashimoto, Y.; Bot, G. P. A.; Day, W.; Tantau, H.-J.; Nonami, H., eds. The computerized greenhouse: Automatic control application in plant production. San Diego: Academic Press; 1993:119-138.
10. Chun, C.; Mitchell, C. A. Dynamic control of photosynthetic photon flux for lettuce production in CELSS. Acta Hort. 440:7-12; 1996.
11. Crawford, S. S.; Pawlowski, C. W.; Finn, C. K. Power management in regenerative life support systems using market-based control. SAE Technical Paper No. 2000-01-2259. Warrendale, PA: Society of Automotive Engineers; 2000.
12. Drysdale,A.; Fortson, R.; Stutte, G.; Mackowiak, C.; Sager, J.; Wheeler, R. Reliability of biological systems based on CBF data. SAE Technical Paper No. 961498. Warrendale, PA: Society of Automotive Engineers; 1996.
13. Eisenberg, J. N.; Maszle, D. R.; Pawlowski, C. W.; Auslander, D. Methodology for optimal plant growth strategies in life-support systems. J. Aero. Eng. 8(3): 139-147; 1995.
14. Eisenberg, J. N.; Pawlowski, C. W.; Maszle, D. R.; Auslander, D. System issues for controlled ecological life support systems. Life Support Biosphere Sci. 1:141-157; 1995.
15. Fleisher, D. H. Crop modeling for multiple crop production and control in Advanced Life Support Systems. Ph.D. dissertation, Rutgers University; 2001.
16. Henninger, D. L. Life support systems research at the Johnson Space Center. In: Ming, D. W.; Henninger, D. L., eds. Lunar base agriculture: Soils for plant growth. American Society of Agronomy; 1989:173-191.
17. Hoff, J. E.; Howe, J. M.; Mitchell, C. A. Nutritional and cultural aspects of plant species selection for a regenerative life support system. NASA-CR Publication 166324; 1982.
18. Hogan, J. A.; Cowan, R. M.; Joshi, J. A.; Strom, P. F; Finstein, M. S. On the development of advanced life support systems maximally reliant on biological systems. SAE Technical Paper No. 981535. Warrendale, PA: Society of Automotive Engineers; 1998.
19. Hopper, D. A.; Stutte, G. W; McCormack, A.; Barta, D. J.; Heins, R. D.; Erwin, J. E.; Tibbitts, T. W. Crop growth requirements. In: Langhans, R. W.; Tibbitts, T. W., eds. Plant growth chamber handbook. North Central Regional Research Publication No. 340. Iowa State University; 1997:217-225.
20. Jones, H.; Cavazzoni, J. Top-level crop models for advanced life support analysis. SAE Technical paper No. 2000-01-2261. Warrendale, PA: Society of Automotive Engineers; 2000.
21. Loomis, R. S.; Conner, D. J. Crop ecology: Productivity and management in agricultural systems. Cambridge Univ. Press; 1996:257-288.
22. MacElroy, R. D.; Tremor, J.; Bubenheim, D. L. The CELSS research program: A brief review of recent activities. In: Ming, D. W.; Henninger, D. L., eds. Lunar base agriculture: Soils for plant growth. American Society of Agronomy; 1989:165-171.
23. Seginer, L; Buwalda, F.; van Straiten, G. Nitrate concentration in greenhouse lettuce: A modeling study. Acta Hort. 507:141-148; 1998.
24. Seginer, L; Oslovich, I. Optimal spacing and cultivation intensity for an industrialized crop. Agric. Systems 62:143-157; 1999.
25. Tadikonda, S. S. K.; Baruh, H. Pointwise-optimal control of robotic manipulators. J. Dynamic Systems, Measure. Control 110:210-213; 1988.
26. Volk, T.; Bugbee, B.; Tubiello, F. Phasic temperature control appraised with the CERES-WHEAT model. Life Support Biosphere Sci. 4:49-54; 1997.
27. Volk, T.; Bugbee, B.; Wheeler, R. M. An approach to crop modeling with the energy cascade. Life Support Biosphere Sci. 1:119-127; 1995.